

Voltage activation and hysteresis of the non-selective voltage-dependent channel in the intact human red cell

Poul Bennekou^{a,*}, Trine L. Barksman^a, Lars R. Jensen^a,
Berit I. Kristensen^a, Palle Christophersen^b

^a*The August Krogh Institute, University of Copenhagen, Universitetsparken 13, DK-2100 Copenhagen, Denmark*

^b*NeuroSearch A/S, Pederstrupvej 93, DK-2750 Ballerup, Denmark*

Received 30 May 2003; accepted 28 August 2003

Abstract

Suspension of intact human red cells in media with low chloride and sodium concentrations (isotonic sucrose substitution) results in strongly inside positive membrane potentials, which activate the voltage-dependent non-selective cation (NSVDC) channel. By systematic variation of the initial Nernst potentials for chloride (degree of ion substitution) as well as the chloride conductance (block by NS1652), and by exploiting the interplay between the Ca^{2+} -permeable NSVDC channel, the Ca^{2+} -activated K^{+} channel (the Gárdos channel) and the Ca^{2+} -pump, a graded activation of the NSVDC channel was achieved. Under these conditions, it was shown that the NSVDC channels exist in two states of activation depending on the initial conditions for the activation. The hysteretic behaviour, which in patch clamp experiments has been found for the individual channel unit, is thus retained at the cellular level and can be demonstrated with red cells in suspension.

© 2003 Elsevier B.V. All rights reserved.

Keywords: Human red cells; Non-selective voltage-dependent cation channel; Ca^{2+} -transient; Hysteresis

1. Introduction

When human red blood cells (hRBC) are suspended in depolarising Ringers, they respond by opening a non-selective voltage-dependent cation pathway, the NSVDC channel, which is permeable to mono- and divalent cations [1–3]. In patch clamp experiments on excised hRBC inside-out patches, bathed in salt solutions of physiological ion strength, depolarising potentials result in opening of a 30-pS channel [4]. At high positive potentials, +100 mV and above, the channel attains an open state probability of close to 1.0. However, the kinetics of the channel cannot be represented by a simple closed to open transition, since the open state probability depends not only on the instantaneous potential, but also on the prehistory of the channel [5,6]. If the voltage is increased from deactivating (negative) potentials towards positive potentials, the open state probability is lower at a given potential, than compared to a

change from positive potentials, at full activation, towards negative potentials. This hysteresis is thus a property of the individual channel unit.

The number of channels in the intact hRBC has been estimated to be in the range of 150–300 [7]. Marked differences with regard to activation seem to exist compared to the isolated channel, but the hysteretic behaviour appears to persist as an ensemble property of the intact cells in suspension. Calcium added to the cells, following activation of the NSVDC-pathway by suspension in sucrose Ringers, results in a hyperpolarization due to activation of the Ca^{2+} -activated K^{+} channels, the Gárdos channel, which deactivates the NSVDC channel. As a consequence of the deactivation, the Ca^{2+} -influx ceases and the active extrusion of cellular calcium by the calcium-pump deactivates the Gárdos channel. Due to the closing of the conductive cation pathways, the conductive chloride pathway becomes more and more dominating, resulting again in positive membrane potentials, which in turn reactivates the NSVDC channel. In contrast to the original activation, from high positive potentials, the activation now takes off from negative potentials and the cation conductance becomes

* Corresponding author. Tel.: +45-35-32-16-83; fax: +45-35-32-15-67.
E-mail address: pbennekou@aki.ku.dk (P. Bennekou).

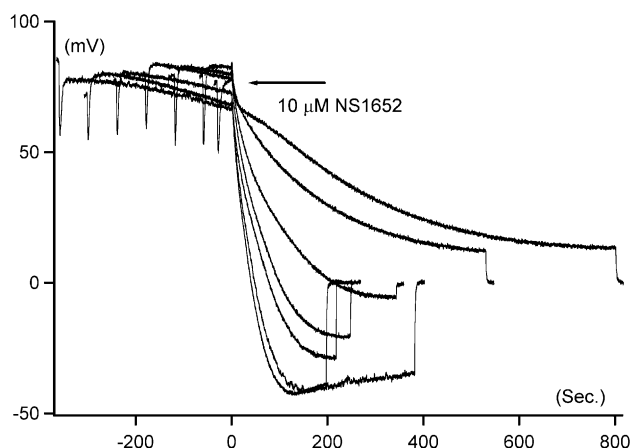


Fig. 1. Delayed addition of NS1652. Initial Nernst potentials in sucrose Ringer are estimated to be: $E_{\text{Cl}} = +105$ and $E_{\text{K}} = -110$. NS1652 was added at time 0. X-axis: time in seconds. Y-axis: CCCP-estimated membrane potential.

lower than before, even at more positive potentials [8]. In the following, a further characterization of the voltage activation and hysteretic properties at the level of the intact cell will be given.

2. Materials, methods and calculations

2.1. Reagents

Carbonylcyanide-*m*-chloro-phenyl-hydrazone (CCCP) (Sigma) and 2-(*N'*-trifluoromethylphenyl)ureido)benzoic acid (NS1652) synthesized at NeuroSearch [9] were prepared as stock solutions in DMSO. Salts and sucrose (Sigma) for the Ringers were of analytical grade or better. Sucrose Ringer, 2 mM KCl, 264 mM sucrose, *n*-Ringer, 154 mM NaCl, 2 mM KCl.

2.2. Erythrocytes

Blood from healthy human donors (the authors) was drawn into heparinized vacuum tubes, centrifuged, the buffy coat and plasma removed, and the packed cells stored on ice until use.

2.3. Experiments

A total of 3000 μl experimental solution was thermostated at 38 °C, CCCP (final concentration 20 μM) and, where indicated, NS1652 (final concentration 10 μM) was added. The experiment was initiated by injection of 100 μl packed cells into the medium giving a final cytocrit of 3.2%.

2.4. Membrane potential estimation

The membrane potential was estimated from the CCCP-mediated pH-change in the buffer-free extracellular solution

[10]. The zero potential (intracellular pH) was determined as the pH in the Triton X-100 lysed cell suspension, as

$$V_m = 61.5 \text{ mV} * (\text{pH}_{\text{in}} - \text{pH}_{\text{out}}) \quad (1)$$

2.5. Conductances

The total membrane current, I_m , due to the passive electrogenic pathways, which is the sum of all the ion currents is given by:

$$I_m = \sum_{i=1}^n i_i = C_m \frac{dV_m}{dt} + \sum_{i=1}^n g_i (V_m - E_i) = 0 \quad (2)$$

where n is the number of individual, discernible conductive pathways, i_i the individual ion currents and C_m the membrane capacitance. V_m , g_i and E_i have their usual meaning. Since $dV_m/dt \ll 1$, the cation conductance can be expressed as:

$$\left(g_{\text{K}^+} + g_{\text{Na}^+} \frac{V_m - E_{\text{Na}^+}}{V_m - E_{\text{K}^+}} \right) = g_+ = g_{\text{Cl}} \frac{E_{\text{Cl}} - V_m}{V_m - E_{\text{K}^+}} \quad (3)$$

3. Results

Initially, when cells are incubated in a sucrose Ringer in the absence of a chloride conductance blocker, the membrane potential has a value corresponding to the chloride Nernst potential (105 mV), which can be calculated from the intracellular Cl^- concentration (100 mM) estimated from the membrane potential measured in *n*-Ringer. The NSVDC channels begin to activate and the membrane potential settles around 80 mV, from which it changes only slowly in the negative direction, due to the still dominating chloride

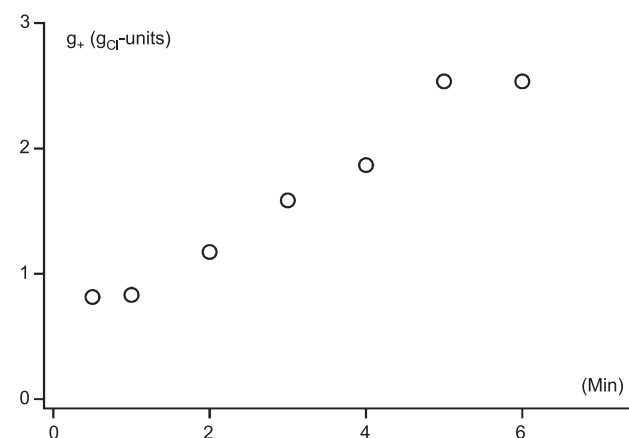


Fig. 2. Delayed addition of NS1652. NSVDC-channel conductance calculated from Eq. (3), as function of quasi-stationary voltage clamp. X-axis: lag time before NS1652 addition. Y-axis: cation conductance in g_{Cl} units.

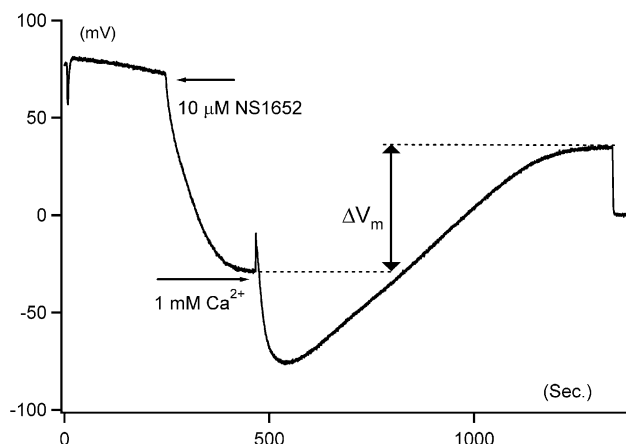


Fig. 3. Ca^{2+} -induced potential transient. Experimental conditions as in Fig. 1. A total of $10 \mu\text{M}$ NS1652 was added after 4 min. When a stationary potential of -28.5 mV was reached, 1 mM CaCl_2 was added. The peak potential was -76 mV and the final stationary potential was $+35 \text{ mV}$. X-axis: time in seconds. Y-axis: membrane potential in mV.

conductance, see Fig. 1. When $10 \mu\text{M}$ of the chloride conductance blocker NS1652 is added, the rate of change of the membrane potential becomes faster and reaching either a peak or a stationary value after a period of time, depending on the lag time before addition of the chloride conductance blocker. The size of the hyperpolarization, reflecting the degree of cation conductance increase, depends too on the lag time, becoming bigger the longer the lag time, see Fig. 2. Adding calcium after the membrane potential has become constant results in a transient hyperpolarization, followed by a new stationary membrane potential, more positive than before the potential transient, see Fig. 3, signifying that the cation conductance is lower after the hyperpolarization.

The hyperpolarization caused by addition of calcium is a graded response, depending on the calcium concentration and the initial depolarization, which was regulated by the

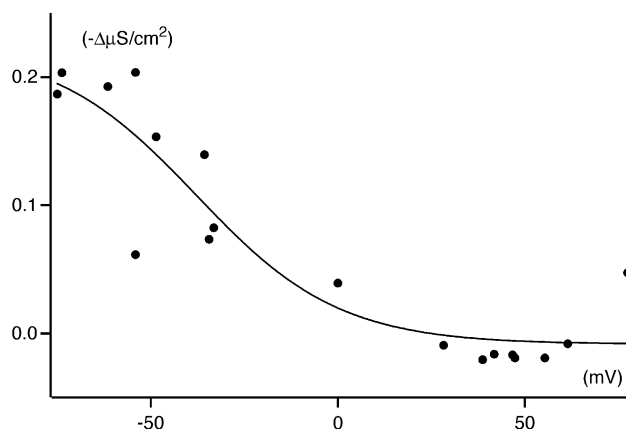


Fig. 4. Channel deactivation by transient hyperpolarization. X-axis: membrane potential in mV at the peak of the hyperpolarization. Line drawn by phenomenological fit to a sigmoid function. Y-axis: conductance change after Ca^{2+} -induced hyperpolarization relative to control experiments, where Mg^{2+} was added ($g_{+(\text{Ca})} - g_{+(\text{Mg})}$).

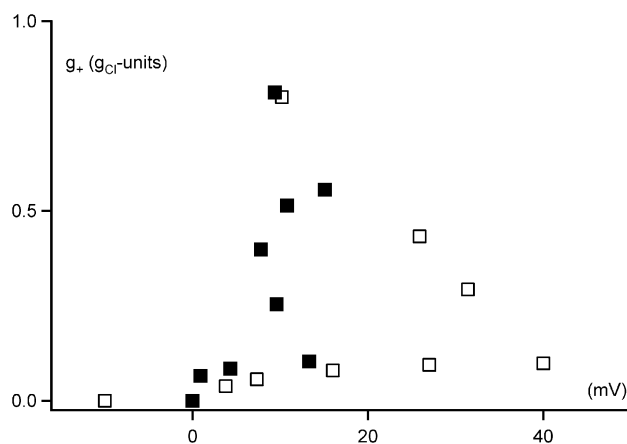


Fig. 5. Depolarization induced channel activation. X-axis: final membrane potential in mV, Y-axis: cation conductance in g_{Cl} units. Open symbols: cells injected into premixed Ringers, filled symbols: preincubation (2 min) in sucrose Ringer, diluted to final composition.

degree of chloride substitution. Fig. 4 shows the difference in conductance after calcium hyperpolarizations compared to parallel experiments where Mg^{2+} was added instead of Ca^{2+} , as function of the peak membrane potential of the hyperpolarization. It is seen that only negative peak potentials result in a conductance decrease after hyperpolarization. It should be noted, however, that the initial depolarization varies between the experiments, due to changes in the degree of substitution.

In order to test the influence of the initial depolarization, experiments were performed, where the degree of chloride substitution was varied, either by adding *n*-Ringer to cells incubated in a sucrose Ringer or by suspending the cells directly in Ringers identical to the final composition in the first series of experiments. The resulting cation conductances vs. the stationary membrane potentials are shown in Fig. 5. Fig. 6 shows the conductances vs. the final chloride Nernst potentials. As demonstrated in Fig. 6, the cation

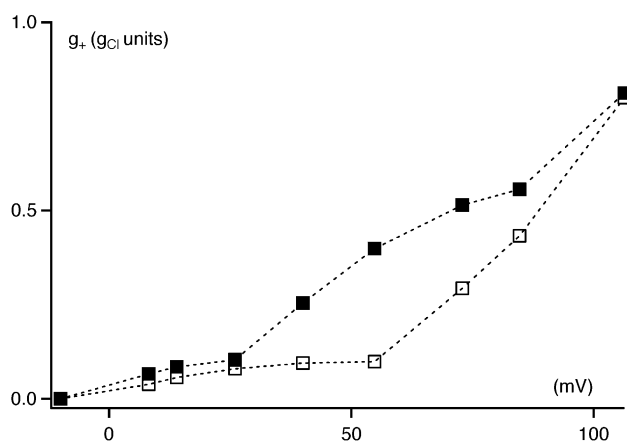


Fig. 6. Depolarization induced channel activation. X-axis: final chloride Nernst potential in mV. Y-axis: cation conductance in g_{Cl} units. Open symbols: cells injected into premixed Ringers, filled symbols: preincubation of cells (2 min) in Ringer diluted to final composition.

conductances calculated for cells preincubated in sucrose Ringer was consistently higher than for cells, which had been directly injected into solutions with higher Cl^- concentrations, and consequently initially less depolarized.

4. Discussion

A major obstacle for the comparison of results from patch clamp studies with experiments on voltage-activated channels in intact cells in suspension is the lack of control with regard especially to the membrane (clamp) potentials. As demonstrated both for the isolated channel [9] and the intact cells in suspension, the conductance changes caused by activation of the NSVDC channel are a function of both time and potential (Figs. 2 and 5, open symbols).

Initially, when human red cells are suspended in sucrose Ringers containing only low concentrations of KCl, the membrane potential attains a value identical to the positive chloride Nernst potential. Over time, the membrane potential changes towards more negative values, due partly to activation of the NSVDC channels and partly to the dissipation of the potassium and chloride gradients. With a normal chloride conductance of about $20 \mu\text{S}/\text{cm}^2$, the salt loss from the cells is considerable, although the membrane potential is fairly constant (quasi-voltage clamp). With the chloride conductance reduced to about $2 \mu\text{S}/\text{cm}^2$ in the presence of $10 \mu\text{M}$ NS1652 [11], the salt loss is reduced (quasi current clamp), but the membrane potential changes in the negative direction relatively fast. The experiments where the cells are incubated in sucrose Ringer, and the chloride conductance blocker is added after a lag time (Fig. 1), show that the longer the cells have been ‘voltage-clamped’ the higher the resulting cation conductance. It should be noted, however, that the increased activation is ‘remembered’, since it results in a more negative membrane potential, which should be deactivating. Compared to patch clamp experiments [6,9], which were, however, done at room temperature and at higher salt concentrations, the time course seems to be somewhat slower, but of the same order of magnitude. With regard to the deactivation, the difference is pronounced. The isolated channel deactivates after an instantaneous jump to negative potentials, with a halftime of about 15 ms [9], whereas the activated channels in the intact cell remain open for minutes, even at moderately negative potentials, and only at very negative potentials they seem to begin to deactivate.

Very negative transient membrane potentials can be attained by addition of Ca^{2+} to cells where the NSVDC channels have been sufficiently activated to allow Ca^{2+} to permeate, thereby selectively increasing the potassium conductance further by activation of the Gárdos channel (see Fig. 3). The hyperpolarization to -75 mV indicates that no appreciable degradation of the chloride and potassium gradients have occurred during the voltage clamp period. However, since the Nernst potential changes due to the

degradation are in opposite directions, the calculation is relatively insensitive to a moderate loss of cellular KCl. This hyperpolarization seems to deactivate the NSVDC channel, thus decreasing the Ca^{2+} -entry concomitant with a delayed [12] active extrusion of cellular calcium by the Ca^{2+} -pump, leading to deactivation of the Gárdos channel. Since the total cation conductance decreases during this sequence of events, the cells are depolarized again due to the persistent positive chloride Nernst potential. This in turn reactivates the NSVDC channel, but in a different state of activity, with a lower conductance reflected in a more positive potential than before the potential transient (Fig. 3). This mode of operation seems to be a parallel to the hysteretic behaviour of the isolated channel, where a plot of the open state probability vs. the clamp potential has two ‘legs’: a low activity state when the clamp potential goes from negative towards positive values and a high activity state going from positive to negative values. This is further supported by differences in conductance seen at identical final sucrose substitutions, but resulting either from activation from very positive membrane potentials showing a high activity compared to the lower activity seen when the channel has been activated at less positive potentials. It is apparent from Fig. 5 that there is no simple correlation between the NSVDC channel conductance and the stationary membrane potential. If, however, the channel conductance is plotted against the final chloride Nernst potential (Fig. 6), the two activity states become evident. Although not a hysteresis curve proper, since the activity is plotted against the resulting chloride Nernst potential, Fig. 6 reflects the memory effect at the cellular level.

Given the estimated number of 150–300 NSVDC channels in a red cell [7] and a single channel conductance of 30 pS at physiological salt concentrations [6], the maximum conductance observed in intact red cells indicate either a very low open state probability, in the order of 10^{-3} or a far lower unit conductance than observed in the isolated channel. The explanation is not known at present, but given the size of the KCl loss, which can be observed and the changes in estimated membrane potential a fraction of cells close to 1 will participate in the response.

5. Conclusion

The hysteresis, which is a property of the individual NSVDC channel unit, is retained as an ensemble property in the intact human red cell. The deactivation of the channel at negative potentials, which for the isolated channel is in the millisecond range, is slower, persisting for minutes.

Acknowledgements

Gurli Bengtson, Hanne Lauritzen and Søren L. Johansen are gratefully acknowledged for their expert assistance.

References

- [1] H. Dawson, Studies on the permeability of erythrocytes: VI. The effect of reducing the salt concentration in the medium surrounding the cell, *Biochem. J.* 33 (1939) 389–401.
- [2] W. Wilbrandt, H.J. Schatzmann, Changes in the passive cation permeability of erythrocytes in low electrolyte media, in: G.E.W. O'Connor, C.M. O'Connor (Eds.), *Ciba Foundation Study Group*, vol. 5, J & A, Churchill, London, 1960, pp. 34–53.
- [3] J.A. Halperin, C. Brugnara, M.T. Tosteson, T. Van Ha, D.C. Tosteson, Voltage-activated cation transport in human erythrocytes, *Am. J. Physiol.* 257 (1989) C986–C996.
- [4] P. Christophersen, P. Bennekou, Evidence for a voltage-gated, non-selective cation channel in the human red cell membrane, *Biochim. Biophys. Acta* 1065 (1991) 103–106.
- [5] P. Bennekou, P. Christophersen, A human red cell cation channel showing hysteresis like voltage activation/inactivation, *Acta Physiol. Scand.* 146 (1992) 608.
- [6] L. Kaestner, P. Christophersen, I. Bernhardt, P. Bennekou, The non-selective voltage-activated cation channel in the human red blood cell membrane: reconciliation between two conflicting reports and further characterization, *Bioelectrochemistry* 52 (2001) 117–125.
- [7] P. Bennekou, The voltage-gated non-selective cation channel from human red cells is sensitive to acetylcholine, *Biochim. Biophys. Acta* 1147 (1993) 165–167.
- [8] P. Bennekou, I. Kristensen, P. Christophersen, The human red cell voltage regulated cation channel. The interplay with the chloride conductance, the Ca^{2+} -activated K^{+} -channel and the Ca^{2+} -pump, *J. Memb. Biol.*, 195 (2003) 1–8.
- [9] International Patent Application WO 98/478779.
- [10] R.I. Macey, J.S. Adorante, F.W. Orme, Erythrocyte membrane potentials determined by hydrogen ion distribution, *Biochim. Biophys. Acta* 512 (1978) 284–295.
- [11] P. Bennekou, O. Pedersen, A. Møller, P. Christophersen, Volume control in sickle cells is facilitated by the novel anion conductance inhibitor NS1652, *Blood* 95 (2000) 1842–1849.
- [12] O. Scharff, B. Foder, Rate constants for calmodulin binding to Ca^{2+} -ATPase in erythrocyte membranes, *Biochim. Biophys. Acta* 691 (1982) 133–143.